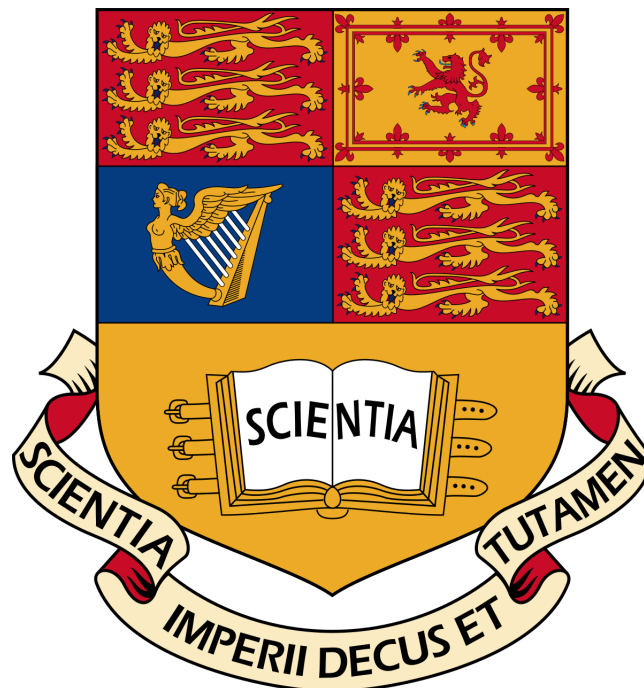


# Variations in Ocean Heat Uptake in the 20th Century

Imperial College London

Department of Physics



Jack T. M. Carlin

CID: 01353253

January 14th, 2020

*Word Count:*  
6076

*Supervisor:*  
Dr Arnaud Czaja  
*Assessor:*  
Dr Heather Graven



# Declaration

I hereby declare that all work henceforth is mine and my partners work only. The work was distributed evenly between us, both inputting into the literature research around the field and the data analysis itself. In my own case, I have previously worked with the supervisor, Dr Arnaud Czaja, on data analysis before, however it was brief work pertaining to atmospheric modelling so this project is not an extension.

# Abstract

---

This dissertation documents Ocean Heat Content trend analysis from 1950 to the present day using the EN4 dataset provided by the Met Office's Hadley Observation Centre. The trend analysis was used to ascertain the rate the ocean is heating or cooling at, and subsequently, deconstructed such that specific trends at certain depths and basins could be compared. The analysis for specific depth ranges and ocean basins was put in context of the mechanisms which are unique to its locality and thus was able to shed light on how local mechanisms are being affected by changing heat content levels in the ocean. It was found that in the last 20 years, the global ocean heat content is increasing at over the double the rate than it was prior to 1998, reaching a rate normalised by the surface area of the Earth of  $0.88\text{W}/m^2$ . Furthermore, this dissertation ascertains that a lot of the heat uptake is occurring in the upper layers of the Pacific Ocean, whilst the source of the greatest heat storage variability is the upper 2000m of the Atlantic Ocean.

---

# Contents

<b>Summary of Work</b>	<b>4</b>
<b>1 Introduction</b>	<b>5</b>
<b>2 Methodology</b>	<b>5</b>
2.1 Layer Methodology . . . . .	6
2.2 Basin Methodology . . . . .	7
<b>3 Results and Analysis</b>	<b>8</b>
3.1 Layer Analysis . . . . .	10
3.2 Basin Analysis . . . . .	12
3.3 Combined Analysis . . . . .	14
<b>4 Discussion</b>	<b>15</b>
<b>5 Conclusion</b>	<b>17</b>
<b>Acknowledgments</b>	<b>17</b>
<b>Bibliography</b>	<b>18</b>

## Summary of Work

In order to gain a better understanding of the oceans, this project was devised to analyse global ocean temperature profiles at different layers of depth, and try to look for trends in areas of warming and cooling; possibly ascertaining if those set areas are changing in their own right. Given the current state of climate change research, it was also deemed valuable to present a position on whether or not this research could be linked to anthropogenic global warming.

This dissertation outlines all of the research conducted, results obtained, and conclusions drawn over the course of five sections. Firstly, the introduction will reiterate the general overview and why there is a need for such research. Then, the next section, the method, will introduce the techniques used to analyse the data. Following the method, the results section will display the execution of the techniques when the data was applied in the form of key values and graphs. Most importantly, the penultimate section will look to discuss those results and draw certain inferences from it; comparing them to the aims we set out the investigation with. Lastly, the concluding section will end the dissertation by providing an overall look at what was achieved, and placing the achievements into the context of the current climate of research.

# 1 Introduction

A growing proportion of the scientific community are looking to answer the question of how our home planet is changing; recent years have moved the spotlight onto climate change, particularly anthropogenic causation. However, the Earth changes regularly despite the changing climate, which can be seen in ocean phenomena, such as El Niño warming events.

This dissertation will look to analyse the changes of the Earth, by honing into its largest surface component, the oceans. To be specific, the heat stored in the world’s oceans, and how that may be changing in quantity and density. Subsequently, the two key questions to be answered are; is the ocean warming, and if so, where is it most prominent?

In order to answer these questions, certain data had to be analysed, and in this case the EN4 dataset from the Met Office Hadley Centre was used. The fourth instalment in the EN data series, the dataset is essentially an amalgamation of subsurface temperature and salinity profiles starting from January 1900. These profiles are obtained from three sources. The majority of the time frame (1900 - 1980) is sourced from the World Ocean Database '13 (WOD13), however between 1990 and 2000, this data is supplemented with profiles collected by the Global Temperature and Salinity Profile Project (GTSPP), whilst the last source adds to the data from 2000 onwards; the ARGO project. Across the three, they get progressively more accurate, with the ARGO dataset being a very thorough profile collection. Despite this, the EN4 amalgamation process puts the collated data through a course of rigorous quality checks to minimise uncertainty and purge duplicates.

Answering the key questions will give us a better understanding of the heat content in the oceans, and how that may change; an inherently valuable property to know for forecasting ocean change. These ocean changes may have a profound impact on ecology and society. Rising ocean temperatures lead to the loss of breeding grounds and coral bleaching, salinity changes, and sea level increases which in turn may cause lethal flooding.

## 2 Methodology

The aforementioned EN4 data came in NetCDF4 format for every recorded month, however the Hadley Centre notes that the data often reverts back to the climatology of 1971-2000 and as such it isn’t suitable for very large trend ranges. Consequently, it was decided that the optimal balance of accuracy and comprehensiveness was to use a range of 1950 to the present. The data was extracted month by month and converted into a four-dimensional array of temperature profiles. The first three dimensions were supplied by EN4 and they indexed latitude, longitude, and depth. The final dimension was a tracker of the month. As a result, we had a longitude-latitude grid for every depth layer and every month.

This longitude-latitude grid was  $360 \times 173$  in size, corresponding to  $360^\circ$  of longitude and  $173^\circ$  of latitude (the latitudes close to the poles were not included). Despite there being 62280 grid-points, some were 'masked', meaning that invalid datapoints would be removed without actually removing the position of the element. Given the nature of the investigation, the invalid positions were the coordinates that described a place on land; when these conditions were met for a point it would return `True` in the masking function and would be invalidated in the dataset. These grids were then layered at each specified depth, of which there were 42. The 42 depth layers were not evenly spaced, instead the difference increased for every layer starting at about 5m of depth, and finishing at  $\sim 5500$ m for the deepest points.

EN4 provided us with global temperature profiles at multiple depths, however temperature

wasn't the key quantity that was analysed. Instead, **Ocean Heat Content** was used, which would give a better view of the energy distribution in the oceans by taking volume elements and quantifying the amount of heat absorbed by it. This was mathematically computed through the integral,

$$c_p \rho \int_z T_{ij}(z) dz \quad (1)$$

where  $c_p$  is the specific heat capacity of seawater at constant pressure,  $\rho$  is the density of seawater, at  $T_{ij}(z)$  is the temperature as a function of depth, which in this case is the temperature at every depth for a gridpoint with coordinates  $(i, j)$ .

Evaluating the integral in *Equation 1* computationally required an interpolation of  $T_{ij}(z)$  because, as mentioned before, the temperature profiles are not equally spaced with depth. To combine the solutions to both tasks, the composite trapezoidal rule was used to linearly interpolate the data and evaluate the integral. Despite the interpolation only being to the first order, the integral is still suitable enough to provide correct magnitude for the Ocean Heat Content (OHC).

After setting up the infrastructure for finding the OHC at a point from the data, the topic plot of the investigation could be obtained; a time series of the raw data, displaying the anomaly in globally summed OHC. This summation was not entirely simple, because it had to be a weighted sum. A gridcell of  $1^\circ \times 1^\circ$  has a larger area near the equator than it does at the tropics. Therefore, in order to weight the sum accordingly the integral had to be corrected for the volume of a sphere, which was realised in a new integral,

$$c_p \rho \iiint_V R_\oplus^2 \sin \theta T_{ij}(z) d\phi d\theta dz, \quad (2)$$

where  $R_\oplus$  is the radius of the Earth, whilst  $d\theta$  and  $d\phi$  are the steps in angle of latitude and longitude respectively. Despite the correction, the integral still wasn't physically viable, as the  $\theta$  in *Equation 2* refers to the angle of latitude from the pole but the conventional use of latitude is the angle from the equator. Subsequently, the angle was changed from  $\theta$  to  $\theta - 90^\circ$ ; the trigonometry in the integral can then be changed from  $\sin \theta$  to  $\cos \theta$ , where the  $\theta$  can now be literally interpreted as the angle of latitude from the EN4 dataset.

\* \* \*

*Section 1* introduced the key questions of the investigation, the first of which we were to answer was whether the oceans are warming, and if so, how? A question which the topic plot would be able to shed light upon. Moving forward however, we sought to answer the second question which pertained to the region of the oceans that was contributing the most to increased ocean heat uptake. To do so, we split the investigation into two avenues. The first was to look into how heat changes with depth, and in particular, which region of depth is heating the most. Whereas the other was to focus on the ocean by its basins, comparing which basin is heating up the most and also which is increasing its efficiency of heat storing.

## 2.1 Layer Methodology

Previously, the methodology to obtain the topic plot of the investigation was to sum the energy stored in spherically corrected columns, spanning down to the maximum depth sampled for any specific grid-cell, which would provide an estimate of the total OHC. However, to compare how this varies with depth we chose to find the sum of the energy stored at particular depth layers.



We chose three characteristic depth layers, which encapsulated different parts of the ocean. These were: the subsurface layer from 0 to 700m; the intermediate layer from 700 to 2000m; and the deep layer which spanned 2000m to the maximum depth at a particular gridpoint. The first layer was chosen to represent the mixed layer and the majority of the thermocline. The mixed layer is an umbrella term for the ocean mass adjacent to the air-sea interface which results in heavily windshear-driven mixing; subsequently a relatively uniform density and distribution of temperature and salinity [1]. The depth of the mixed layer varies due to its strong link with sea-level atmospheric conditions, however, research shows that the boundary would not descend lower than 200m which means it is fully encapsulated by the investigation-defined subsurface layer [2]. Beyond the boundary of the mixed layer follows the ocean thermocline, which is a bridging zone from the warmer mixed layer to the colder deep waters where there is an abrupt decline of temperature. By virtue of being in the subsurface layer, it is characteristically seasonal and varies notably with the incident solar flux and atmospheric conditions. The subsequent layer is characterised by being the beginning of the aphotic zone in the ocean; where the ocean is categorised on no longer being affected by predominantly sunlight as only 1% of sunlight reaches the plant-life [3]. Nevertheless, the intermediate layer is still physically dynamic, particularly with overturning circulation, a process where colder deep waters which are part of the thermohaline circulation (THC) go through a vertical mixing and travel towards the equator. So, despite its independence from incident solar radiation, it is a layer which has its motion dominated by large-scale ocean currents, contributing to global ocean heat transport. This is unlike the final deep water layer which is relatively dormant. At its greatest depths, the water is deoxygenated and contains the highest nutrient salts content. Naturally this is where the densest water will be which means that the ocean mixing cycles take the longest amount of time but are still present. In particular with this investigation, it is worth noting that this is where the data profiles are most sparsely sampled so the interpolation will have a larger margin for error.

## 2.2 Basin Methodology

In addition to pinpointing changes in ocean heat uptake with depth, it is also important to analyse how heat content is changing laterally across the globe in different ocean basins to ascertain where this heat content is increasing the most, something this avenue of analysis sought to answer. The basins that were analysed in this investigation were: the North and South Atlantic and Pacific Oceans, the Arctic and Antarctic/Southern Oceans, and the Indian Ocean.

As aforementioned, the data was presented in grid form and thus had no infrastructure for picking out particular ocean basins, and as a result the solution was to functionally cut sections out of the global array. This was done by declaring indices for rectangular sub-arrays of the dataset which would contain the whole basin then to iterate over just those indices when operating for a particular basin; indices that can be seen in Table 1. This proved effective because the data was masked at land cells, therefore a conditional could be set to only operate on unmasked array values; circumventing any issues raised by choosing large sub-arrays which encompass a lot of landmass. Additionally, when these grid cells are parsed over, their spherically corrected area is recorded then summed after the total operation to find an estimate of the surface area of our working basin.

Basin	Longitude Range	Latitude Range
Arctic Ocean	0° - 360°	66°N - 86°N
North Atlantic	53°W - 5°E	0° - 66°N
South Atlantic	70°W - 19°E	63°S - 0°
North Pacific	180°W - 81°W	0° - 66°N
South Pacific	180°W - 81°W	63°S - 0°
Indian Ocean	19°E - 119°E	63°S - 10°N
Southern Ocean	0° - 360°	86°S - 63°S

A different method which was also employed to investigate the heating or cooling of basins, is to plot heat content trends at a particular grid-cell, as opposed to looking at total OHC in a basin. This is important so that certain cross-basin phenomena are not simply missed, such as the effects of pressure anomalies over the Eastern Pacific and over Indonesia during an El Niño event causing strong localised heating. Consequently, it was decided to show global trends which required the fitting of linear functions over the time series of heat content at a particular point. For a gridcell, the OHC was plotted against the time-frame, and a Levenberg-Marquardt least-squares algorithm was used to minimise the function into a line, from which the slop was recorded.

Regardless of the method to look at the changes to heat content in a basin, it is highly important in not only investigating the whereabouts of the largest regions of ocean heat uptake, but also to look at the relationship between geographical locality and heat uptake changes. One key item of context going into the investigation is that the Pacific is typically 'fresher' than the Atlantic, meaning that the salinity is lower on average, however there are various other mechanisms that are unique to specific basins; the prominence of sea ice in the Arctic Ocean, or the plausible volatility that may arise due to the Antarctic Circumpolar Current (ACC).

### 3 Results and Analysis

The production of the results follow the rough chronology that was outlined in the methodology with certain additions and changes that were realised throughout the analysis process. Despite that, the first key result to analyse was still the topic plot, shown in *Figure 1*, which was the overall trend of the data in the form of Ocean Heat Content.

It specifically outlines the Ocean Heat Content anomaly which was calibrated by using the mean of the OHC level from 1950 to present. The data trend shows that there was a steady increase from the mean throughout the 20th Century, but at the turn of the 21st Century, there is a very large divergence from the average. As outlined previously, the data is heavily oscillatory due to nature of the Earth's seasons, however it is also worth noting that the amplitude of the oscillation seems to decrease from 2000 onwards, which may be due to the amalgamation of ARGO; a dataset that was the dominant contributor to the data of the 2000s for EN4, thus less data assimilation could result in a smaller variability. It is also plausible that the increased heating effect would mask the variability. In order to quantitatively investigate the large increase in ocean heating, we could extract a rough estimate of the general slope of the anomaly by using a similar least-squares fitting introduced in *Section 2* to assign a linear fit to the data. However, for the sake of comparing this heating gradient to a wide array of literature sourced values, we had to normalise with the surface area of the Earth so that it could be contrasted to satellite heat flux values. Consequently, the total normalised heating gradient from *Figure 1* was  $0.349 \pm 0.042 W/m^2$ , however when the data was constrained solely to a period of 1998 to present, the slope was  $0.88 \pm 0.064 W/m^2$ , thus exhibiting over two-and-

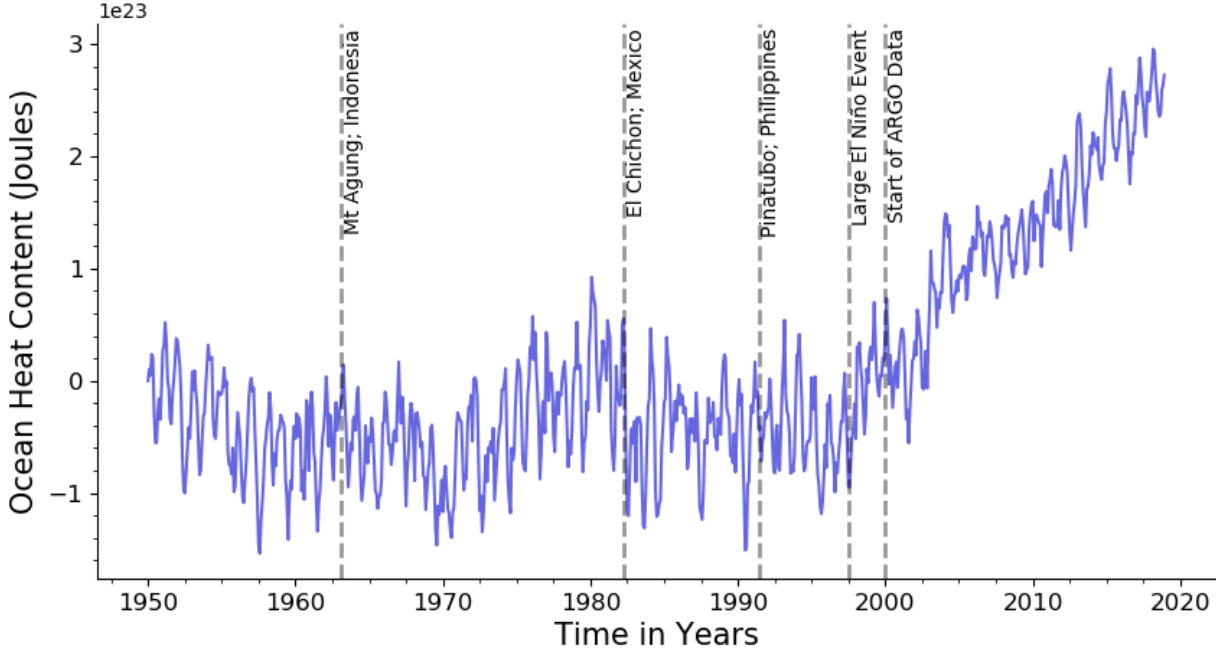


**Figure 1:** The plot displays the OHC anomaly against years. This anomaly was obtained by subtracting the 68 year mean from the data. The dashed lines show events which were significant enough to pertain to OHC levels and thus would corroborate with the form of the raw data.

a-half times the heating in recent years, which would corroborate with recent conclusions of increased planetary warming [4] given that the global oceans act as the largest heatsink.

Furthermore, there are other key conclusions to extract from the topic plot, in particular the effect certain global events have on Ocean Heat Content. The modal event on *Figure 1* is a volcanic eruption, three of which occurred within the investigations time range that were suitable impactful on the oceans heat content. Volcanic eruptions have the largest impact on heat content within the very shallow depths, and specifically on sea-surface temperatures (SSTs) so they may not be the most pronounced on the topic plot. Despite that, the most obvious effect is the eruption of El Chichón, in Mexico, in 1982 where the heat content appears to drop by  $1 \times 10^{23} J$ . According to an investigation on the impact of volcanic eruptions in 2005, El Chichón was the second most impacting eruption of the century behind the Mount Pinatubo eruption of 1991 (also displayed on the plot), which decreased the global oceanic heat content by  $3 \times 10^{22} J$  [5]; a whole order of magnitude smaller. This would imply that the majority of the abrupt decrease of the early 80s in *Figure 1*, came about to other coinciding effects such as the 1983 La Niña cooling.

On the other hand, this effect may be more prominent in *Figure 2*, below, which shows the heat content time series over the same range up until 1000m depth. This metric does not link with the characteristic layers that were defined as it is not part of the layer analysis; instead, it is to show the existence of the error bars for the EN4 dataset. As aforementioned, EN4 only publish error bars for the temperature profiles up to 1000m, thus *Figure 2* serves the purpose of looking at the extent of the errors and how they vary over time. As expected the magnitude of the total error decays with time, fitting in with how EN4 outlined their error reanalysis methodology, which is to assign to an extrapolated point based on how geographically close it is to an observed point [6]. Accordingly it matches with the increasing number of expendable bathythermograph (XBT) obtained profiles that are within the dataset. Nevertheless, it is still likely that the error is an underestimate of what the true qualitative error is. This is because there is an error associated with the data taking process in the form of a time bias, the

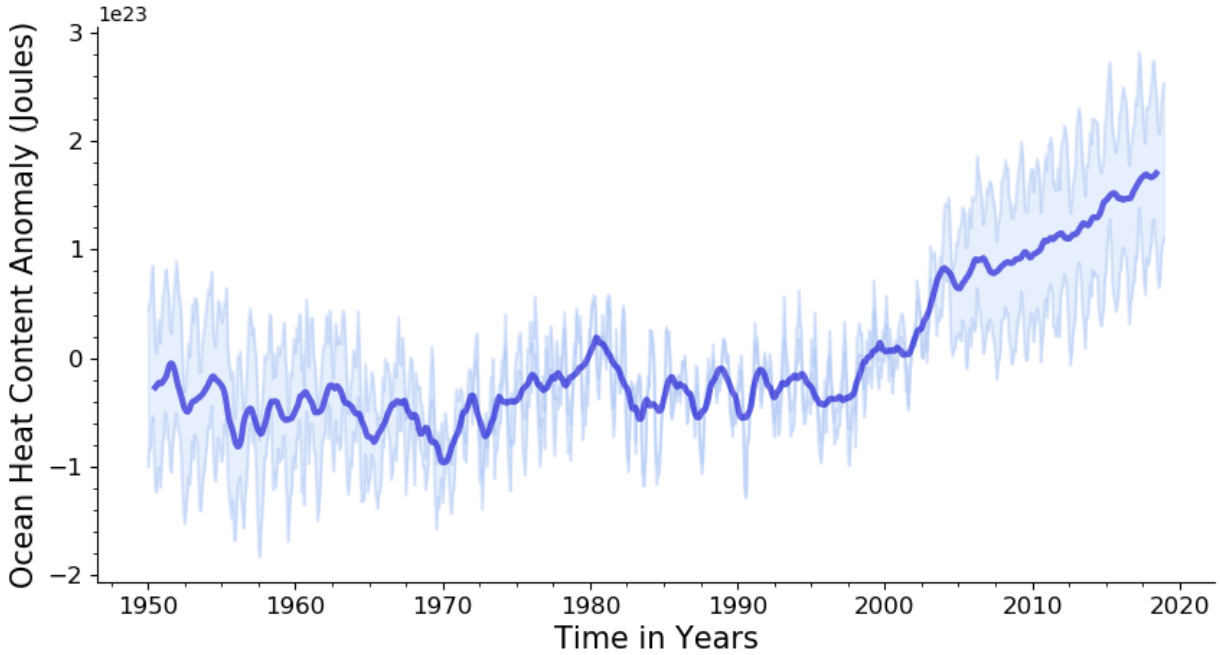


**Figure 2:** A continuous error bar is overlaid with the 12 month moving average of the unperturbed data. These error bars were calculated by shifting the data by adding and subtracting the maximum error at a point to find the two extremities of the data.

XBTs used to take the data do not return their physical location, only the profile data, and as a result time and estimated velocity of decent are used for an approximate position. Once ARGO achieved full coverage in 2003, the magnitude of the uncertainty seems to shoot up and stay roughly constant, which may be due to ARGO having a better estimate of the actual error involved with recording the ocean profiles. This is helpful for extracting more truthful values, with indicative error ranges, however uncertainties are still only present down to 1000m, constraining error propagation.

### 3.1 Layer Analysis

The first order of analysis past the topic plot was the layer analysis and was analysed under a similar scope as the total heat content, with the exception that now the integral was evaluated down to specific depths. *Figure 3* shows the OHC anomaly for each layer on the same plot and thus how they can be proportionally compared.

It is clear from the figure that the top two layers are increasing at steady rates respective to their layer, with the subsurface layer increasing at the largest rate and displaying the largest abrupt rise in the early 2000s. Conversely, the deep layer shows very little change over the whole time period, with the majority of the time just oscillating with very small net changes. It has however, showed a small but steady incline beginning in around 2013, which could be an indicator of recent deep-water heat uptake but the statistical confidence of that claim is questionable until more years of data is collected.

Before the large heating period of recent years, the subsurface shows very strong variability especially in the 60s and 80s; as much as to change by  $5 \times 10^{22}$  within 5 years. This volatility is probably dominated by its strong link with atmospheric conditions which would have been varying from year to year depending on various external factors like the aforementioned volcanism, El Niño-Southern Oscillation (ENSO), or even the sudden influx of aerosol injection

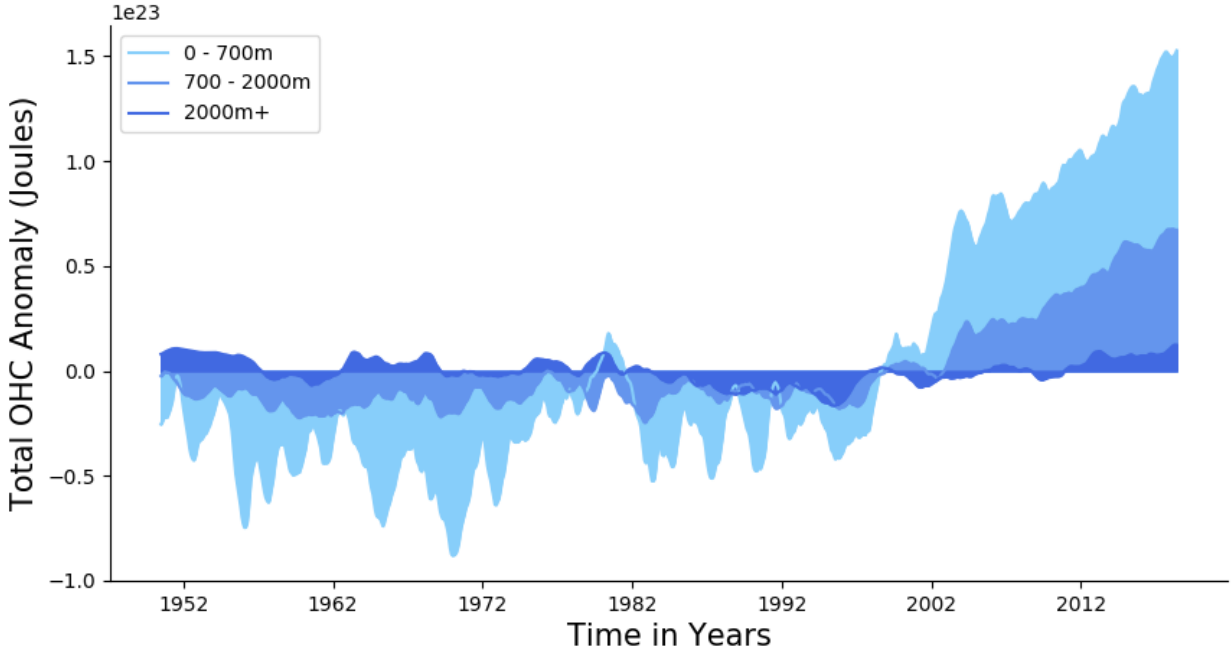


**Figure 3:** An anomaly plot where the reference point was the 68 year mean for each layer respectively. A 12 month moving average was used on the anomaly to smooth out the volatility. The anomalies are colour filled to the zero line to compare proportions but the values are still the same as previously shown.

into the atmosphere. Even though the volatility has led the subsurface layer to its largest anomaly magnitude trough of almost  $-1 \times 10^{23}$  in 1959, it is still clearly the largest contributor to increased ocean heat uptake in the last 20 years. Additionally it is worth noting that the troughs of anomaly prior to the 21st Century will be slightly skewed because the anomaly is calibrated from the mean which would be larger due to the recent heat spike.

In a similar fashion to *Figure 1*, the heat gradient normalised with the global surface area can be extracted for comparisons with data acquired elsewhere, in this case the gradients follow a proportional sequence, the ratios for which can be ascertained from the filled areas in *Figure 3*. The fluxes were:  $0.206 \pm 0.032$ ,  $0.117 \pm 0.011$ , and  $0.026 \pm 0.008 \text{ W/m}^2$  for the subsurface, intermediate and deep layer respectively.

The numbers reflect a strong dominance in the shallow depths of heat content increase. The increasing heat storage in the upper layers of the ocean has been a topic of research recently as the Atlantic Meridional Overturning Circulation (AMOC) is seemingly weakening in strength which is leading to an intense stratification of ocean layers. The AMOC works to flow seawater from the upper layers northward or colder, deeper waters southward, causing a vertical mixing effect; in turn, this helps to distribute the heat density more uniformly across all layers of the ocean. However, due to global warming from the increased presence of greenhouse gases and the increased freshening of the North Atlantic, the currents have weakened so less heat is being distributed [7]. As a result, this may be a suitable explanation for how the disproportionate heating occurring in the upper layer in contrast to the layers below with the uppermost layer heating at almost double the rate of the next layer just 700m below. Furthermore, this could also lead to a violent runaway effect where global warming increases the heat content of the ocean which would cause a freshening effect from sea level rise leading to an even weaker AMOC.

### 3.2 Basin Analysis

As we have seen, the properties of different ocean basins have a large role in determining how heat is transported and distributed across the ocean. We can see that this is why analysis of ocean basins is strongly warranted in order to fully understand changes in ocean heat uptake, by contextualising the dynamics of each basins heating or cooling effects with certain mechanisms unique to that basin in particular. By following the same vein of analysis in the previous section, *Figure 4* shows the OHC anomaly plot for all seven basins outlined in *Section 2*. There is a distinct change, however, between *Figure 4* and *Figure 3*, where in this case the heat content is summed over a certain basin to the maximum depth, but then it is normalised by the basins area. This means that the anomaly is in  $J/m^2$ , and instead of just being an OHC anomaly, it is an efficiency term of heat content per unit area so we can investigate which basin is increasing its capacity to store heat the most to look out for later stratification, analogous to the thinning of heat storage in the North Atlantic.

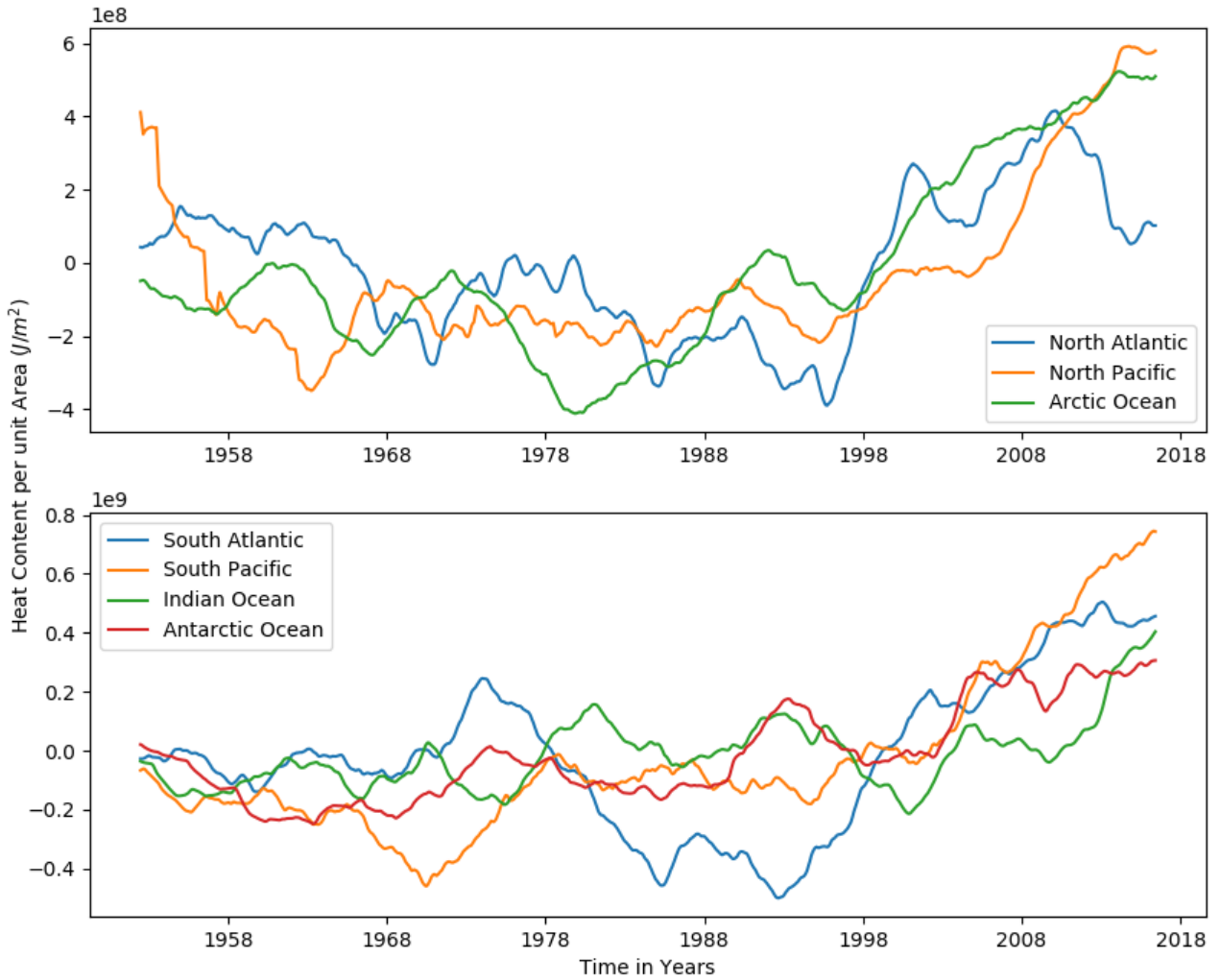


**Figure 4:** The OHC per unit Area anomaly is split into two sub-plots, the top plot shows Northern Hemisphere basins whilst the bottom shows those in the South. This was done for clarity as there are many line plots. Additionally the moving average is increased from 1 year to 5 years for this reason as well.

Out of all seven basins, the one which has reached the largest OHC per unit area at present day is the South Pacific, reaching  $7.5 \times 10^8 J/m^2$  by 2018. The Pacific in general has also been rising at the largest rate with both the North and the South increasing the most out of their



respective. However, it is worth noting that almost all the basins have had their specific heat content increasing since the 90s, with the exception of the Antarctic Ocean which has been rising steadily all throughout the investigations time period. Overall, this fits in with the previous figures which also show large increases from the 90s, and thus would correspond with the notion of anthropogenic climate change [8]. One prevailing subset of that line of reasoning would help to explain why the Southern Hemisphere seems to be increasing in specific heat content the most. An investigation in 2005 on the human-induced warming of the oceans reasoned that the disparity in atmospheric aerosol density between the Northern and Southern Hemisphere has led southern oceans to increase their heat uptake; the majority of the world's population can be found in the Northern Hemisphere and therefore the presence of aerosols are far stronger [9]. Consequently, the smaller aerosol concentrations over the southern oceans lead to an absence of near-cancelling effects which can be observed in the north [10].

Another key feature of *Figure 4* is the extreme variability of the North Atlantic in specific heat content throughout the whole time period. In correspondence with the previous conclusion drawn from the data, the general trending of the North Atlantic still seems to be increasing however there is a 10 year period oscillation which veils the true trend. This same variability does not appear on the profile for the South Atlantic, which would imply that this effect is the manifestation of the Atlantic Multidecadal Oscillation (AMO), a climate cycle that has a dominant effect on sea surface temperatures, and thus weather effects, in the North Atlantic. The AMO is intrinsically linked with the aforementioned AMOC, as well as temperature variation in the Pacific. In years where the AMO is peaking, there is a similar peak in rainfall which freshens the North Atlantic [11] and may channel into the feedback loop for the AMOC which has a salinity dependence.

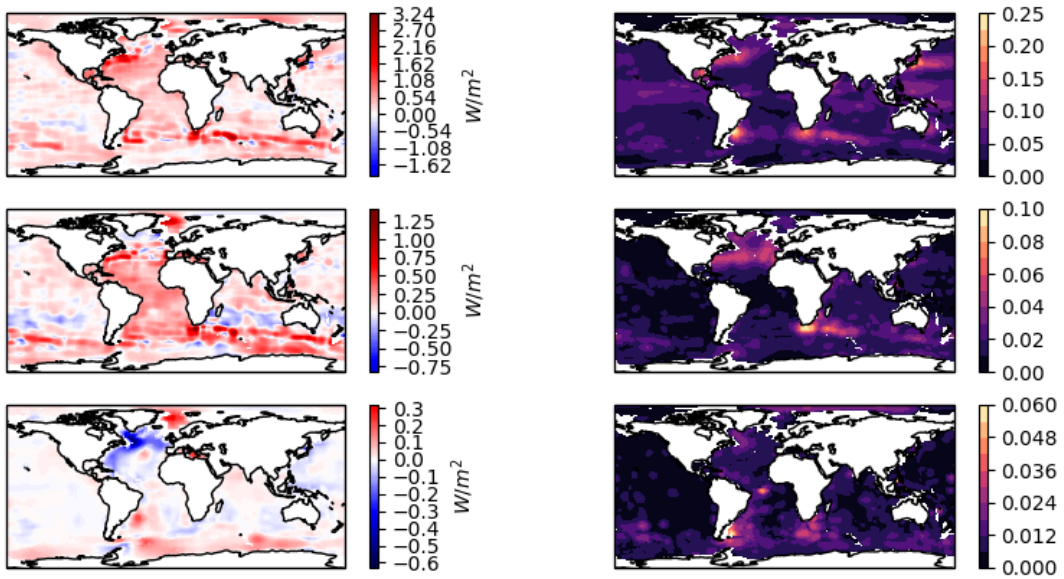


**Figure 5:** The plots on the left display the filled contour plot of the linear OHC trend at every gridpoint, whereas on the right displays the standard deviation of the linear fits used at each point. Every row pertains to the characteristic layer descending in depth range for each row.

The previous forms of analysis included extracting a least-squares-minimised gradient of the trends however in this case the plotted value has changed to a specific heat content. Additionally, the used basins are just estimates as the actual borders are often undefined given that the ocean is a continuum, meaning certain parts of the ocean are not fully represented in *Figure 4*. Therefore, to fully represent the horizontal form of the ocean, the normalised heating gradient was found at every grid cell and overlaid onto the total array as a filled contour map to show

the variation of OHC trends. This contour map is shown in *Figure 5*, and is split into each characteristic layer as well. In addition to just the OHC contribution at every coordinate, there is a parallel set of contour plots which show the standard deviation of the linear fits used at every point, which attempts to display the validity of using a linear fit in the first place.

These contour maps reflect the conclusions drawn so far, such as a great deal of heating in the top layer, variability in the Southern and North Atlantic Oceans, and weak dynamics in the deep layer. An aspect of ocean thermodynamics which is revealed through *Figure 5* is the disproportionate cooling along the North Atlantic Deep Western Boundary Current, shown in the bottom left map. It is possible that this large cooling effect is due to the weakening of the AMOC, which would typically vertically ascend cooler waters along the western boundary further and bring them southward, however with a weaker current the dominant heat transport mechanism would be the simple upwelling of hot water parcels causing further stratification of heat with depth.

The right side maps of *Figure 5* also show an indicative pattern which reinforces previous conclusions, of note, is the variability of the upper layer. Observing the magnitudes of the standard deviations across the whole map, the top layer has the largest average error on the order of magnitude of  $\pm 10^{-1} W/m^2$ . As the layers progress the average uncertainty decreases by about an order of magnitude each time, however at every layer, there are recurring regions of peak uncertainty; whilst areas like the North-Western Pacific seem to dissipate in standard deviation past the subsurface layer, the North Atlantic and the Agulhas always present the smallest confidence in linear fitting. This is expected for two reasons. Firstly, these regions have shown strong variability prior and have key mechanisms which drive it (given the Agulhas area is close to the Southern Ocean). Yet, another reason is that the EN4 dataset has the highest uncertainty in those regions also due to its temperature volatility, as such it works in tandem and results in an amplified effect meaning that a linear fit shows a spiked variance in those regions [6].

The contour plots serve to reinforce inferences made by other plots but more importantly to provide a visualisation of the whole picture in terms of heat content changes. It also begins to entwine the basin and layer analysis by showing lateral OHC trends across the globe but constraining it to the characteristic layers. This was a notion that we sought to build upon by creating an avenue of analysis which manages to combine depth and basin variation into one plot that encapsulates the coupling.

### 3.3 Combined Analysis

To achieve succinct analysis which shows heat variation with depth, unique to a basin we settled on a 'depth penetration' plot. The methodology behind this hinged on using sub-arrays as outlined in *Section 2.2* but this time to record the temperature gradient as opposed to evaluating an OHC integral. The algorithm parsed over every gridpoint in a basin at a particular depth and used least-squares to linearly fit over all temperatures at that gridpoint from 1950 and subsequently find a trend in  $K/yr$ , then after all gridpoints in the specific basin depth have been operated on, the average trend across that whole depth is found and recorded. This repeats over every depth provided by the dataset (42 unevenly spaced depths until 5500m), which is then repeated as a whole process for the seven basins.

*Figure 6* shows the fruition of this analysis with a subplot split into the seven basins. The slopes that were used as the datapoints were not calculated using linear trends from 1950, but rather 1998 in order to try to understand the changes to the basins with depth over the course of the last two decades where the heat content of the oceans has been shown to grow



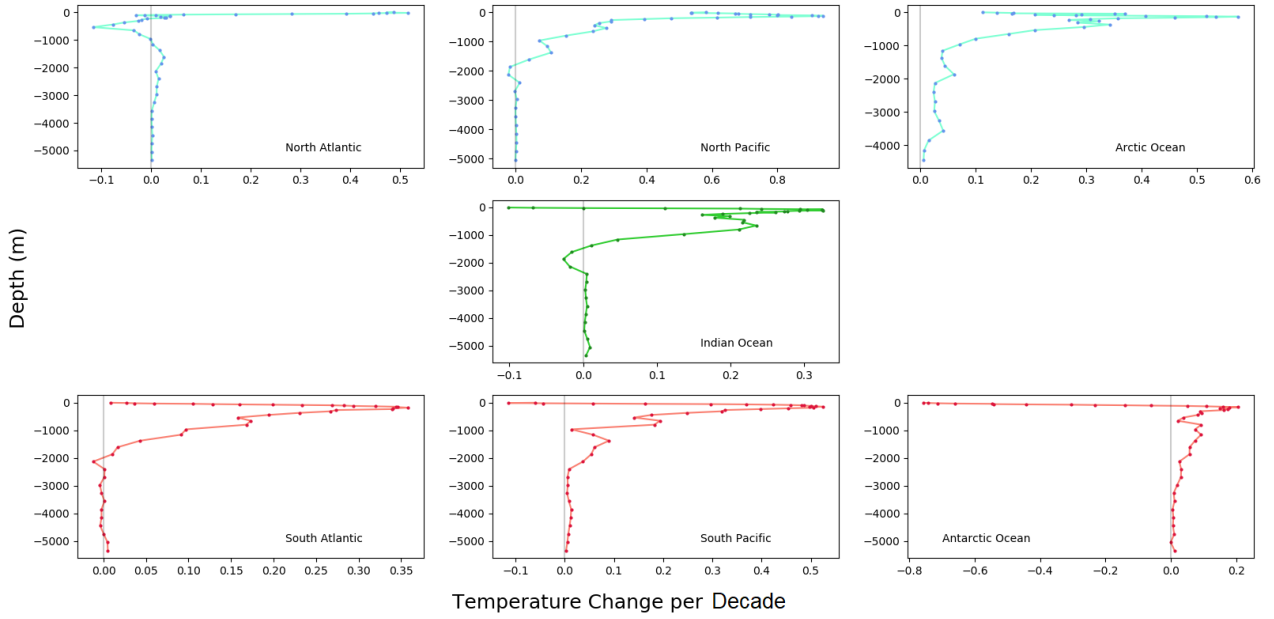


**Figure 6:** This displays seven sub-plots corresponding to each basin. Each subplot shows the relationship between depth and average temperature trend of that basin at the depth in kelvin per decade. Each plot has their own set of sub-axes so the difference in the size of peaks will vary from plot to plot.

rapidly. The figure shows a lot of information, reemphasising previous conclusions as well as revealing possible recent changes to the structure of certain basins. We can still observe the larger heating rates in the pacific, whilst the North Pacific seems to be heating at the largest magnitude at a certain layer, the South Pacific has a deeper penetration of heat which likely results to a larger overall change in OHC. This recent North Pacific heating is also reflected in the change in the SSTs across the whole basin. A study conducted in 2016 looked at the SST trend between 2002 and 2012 and found that the North Pacific peaked at some points at 1.5K per decade, which in turn would correspond to our values of 0.6-0.8K per decade just below the surface [12]. Additionally the plot may also strengthen the argument that vertical mixing in the North Atlantic is weakening over time causing a stratification effect, as we can see in *Figure 6* all of the positive temperature gradients are confined to the 0-700m layer whilst there is a small kick back effect below resulting in cooling from the last 20 years. Lastly, it is worth noting that there appears to be effect of an initial increase of temperature gradient immediately below the surface until a peak, yet intuitively the closest to the surface should face the most extreme heating/cooling effect. One possible explanation for this is that ocean-atmosphere interactions lead to a lifting of heat from the surface of the water body, due to over-passing winds, and thus a temperature gradient is created such that heat is pulled from immediate subsurface depths to the surface, which are not recorded in this dataset.

## 4 Discussion

The investigation has shed light on the changes in heat content of the worlds oceans and how the data may perpetuate that established oceanic mechanisms may also be changing in tandem. The changing trends of OHC levels have been a topic of discussion in the field of physical oceanography for many years now, and many of the methodologies that have been developed are transcendent through multiple papers [13], with slight variations or changes to the data input to further investigate. In particular, the normalised OHC trend is often a metric for

comparison given that it is dimensionally parallel with flux readings from satellite data. As a reminder, the investigation outlined in this dissertation concluded that the numerical total trend in the OHC from 1950 to 2019 was  $0.349 \pm 0.042 \text{ W/m}^2$ , and if this was to be constrained to just the recent years of 1998 to 2019 it increases to  $0.88 \pm 0.064 \text{ W/m}^2$ . Furthermore, if instead it is broken up into the characteristic layers we find that each layer (0-700, 700-2000, 2000+) there is a normalised OHC trend of  $0.206 \pm 0.032$ ,  $0.117 \pm 0.011$ , and  $0.026 \pm 0.008 \text{ W/m}^2$ .

A similar study from January 2019 looked to reconstruct a model of historical global heat storage in a close fashion to this dissertation, whilst using a much larger time period from 1871 to 2017. In this paper, OHC time series were analysed but with multiple different data sets to obtain a more statistically sound estimate on global ocean heating. They focused in on a similar time period to our investigation, 1955-2017, and through this they were able to obtain a total heating trend of  $0.33 \pm 0.057 \text{ W/m}^2$ , which reinforces our findings by only having a mean percentage difference of 5.7%. They went further by looking at depth discrepancies and finding that in the first 700m of ocean depth there is a heating trend of  $0.220 \pm 0.050 \text{ W/m}^2$ , whereas beyond the 700m depth mark the trend they found was  $0.110 \pm 0.007 \text{ W/m}^2$  [14]. Moreover, a study in 2013 was conducted to pinpoint climate signals from ocean heat content reanalysis. They too used OHC trends as a cornerstone analysis metric but split up the trends by decade; consequently it gave us a chance to compare our recent values to their 2000s trend. The study declared their OHC linear trend to be  $0.85 \pm 0.106 \text{ W/m}^2$  using the ORAS4 dataset [15], which also bears striking resemblance to our own with a 3.5% difference.

Overall, it can be seen that the results that were ascertained from the investigation fit into an acceptable range of the current climate of physical oceanography research, but that does not mean that our investigation was free from analytical mistakes and showed key weaknesses throughout. The first and most notable external factor was down to the EN4 dataset itself. As aforementioned, the Hadley Centre does not recommend the use of EN4 for long term trend analysis due to its tendency to relax to climatology for weakly extrapolated gridpoints, and therefore this set an intrinsic constraint on the investigation, as the data could not be analysed from before 1950 to maintain a certain level of integrity. Additionally the errors are only present from the data up to 1000m of depth which meant that all the errors for the values we extracted are just from the confidence level of the least-squares linear fit on the time series. A widely used way to circumvent one poor dataset is to use multiple different datasets which may show a strength where another shows a weakness.

Another pitfall of the investigation comes from the integral in *Equation 2* where the two constants outside the integral represent the specific heat capacity of seawater and the density of seawater. The integral cannot provide a good mathematical representation of the problem because these two are not constants and are functions of depth and temperature in the ocean, particularly density which would have a defined gradient with depth and a defined pycnocline [16]. Making these functions of depth would include them into the integral and create a far more complex model by using more complicated numerical operations for the integration, and thus was deemed outside the scope of the investigation, yet nonetheless it still reduces the accuracy of the heat distribution.

Lastly, the depth layers were unevenly spaced; the spacing increasing as the total depth increased. As a result it was required to interpolate the data to get a more accurate temperature distribution from the dataset, however that was included in the use of the trapezium rule which acts as interpolator of the first order. This method of interpolation is very weak, so even though it may have not changed the order of magnitude of the OHC values, it would produce a non-insignificant error on the values which were not quantified. To rectify a weak interpolation on the data, prior to integrating the data set could have been smoothed out via the use of natural

cubic splines which would iteratively form a cubic function in between the datapoints along the depth axis. Integrating from there would be far more reliable and precise, especially if a Monte Carlo method of integration was used, such as a metropolis algorithm.

## 5 Conclusion

To conclude, the aim of the investigation was to determine whether or not the ocean is heating, and if so, where is this occurring in the largest force. Both questions were answered and along the way, we were able to find plausibly matching mechanisms to describe and justify the presented data. We have been able to ascertain that the most heated vertical region of ocean is the top 700 metres and also attributed a heat stratification with depth effect which may be causing a feedback loop to trap even more heat in the upper layers. Moreover, the ocean basin which seemed to be the largest contributor to an increased ocean heat uptake was the Pacific Ocean in its entirety, specifically the South Pacific. It was also deemed worth noting the variability of certain areas of the ocean; areas which required a larger moving average to determine a linear trend with better confidence. The part of the ocean which was the most variable was the upper 2000m of the North Atlantic. This follows the mechanisms listed in the dissertation which are active in the North Atlantic, of which there are many, and influential enough to cause great variability.

The investigation outlined in this dissertation lays strong groundwork for further research into specific regions of the ocean so that their unique mechanisms can be put into clearer mathematical context, thus forming a stronger mathematical model of our worlds oceans. The combined analysis (layer-wise and basin-wise can be continued for a specific basin to look at how much the vertical transport of heat is varying with time, and possibly link the variable and heating upper layers to ocean-atmosphere interaction dynamics.

In a generation where the general populace are becoming rapidly more aware of the changing climate, it is imperative that the thermodynamics of the ocean are better understood given their overwhelming contribution to the Earth's ecosystem, and we hope that this dissertation would be able to contribute, even a minuscule amount, to this task.

## Acknowledgments

My partner and I would like to thank Dr Arnaud Czaja for setting up a BSc Physics Project outside the scope of what is taught in the undergraduate degree; a fresh and engaging field of physics for us to learn about. We would like to thank him further for his supervision in the project and guidance on how to move forward at points of impeded progress. In addition, we would like to thank Dr Heather Graven, for taking her time to assess us and providing us with feedback to implement in this report. Of course, completing this project to the extent it was would not have been possible for me personally without the expertise of my partner, Callum Duffy, who poured many hours of work into the investigation, along with myself; with many nights spent debugging code, seemingly fruitlessly at the time. Finally, we must thank the Met Office Hadley Observation Centre for equipping us with the tools to carry out such research by allowing public access to the EN4 dataset on their website.

## Bibliography

- [1] A. B. Kara, P. A. Rochford, and H. E. Hurlburt, “Mixed layer depth variability over the global ocean,” *Journal of Geophysical Research: Oceans*, vol. 108, no. C3, 2003.
- [2] D. Swain, M. Ali, and R. A. Weller, “Estimation of mixed-layer depth from surface parameters,” *Journal of Marine Research*, vol. 64, no. 5, pp. 745–758, 2006.
- [3] A. J. Ferreira and R. Siam, “Core microbial functional activities in ocean environments revealed by global metagenomic profiling analyses,” *PLoS One*, vol. 9, no. 6, 2014.
- [4] M. E. Mann, R. S. Bradley, and M. K. Hughes, “Northern hemisphere temperatures during the past millennium: Inferences, uncertainties, and limitations,” *Geophysical research letters*, vol. 26, no. 6, pp. 759–762, 1999.
- [5] J. A. Church, N. J. White, and J. M. Arblaster, “Significant decadal-scale impact of volcanic eruptions on sea level and ocean heat content,” *Nature*, vol. 438, no. 7064, p. 74, 2005.
- [6] S. A. Good, M. J. Martin, and N. A. Rayner, “En4: Quality controlled ocean temperature and salinity profiles and monthly objective analyses with uncertainty estimates,” *Journal of Geophysical Research: Oceans*, vol. 118, no. 12, pp. 6704–6716, 2013.
- [7] L. C. Jackson and R. A. Wood, “Timescales of amoc decline in response to fresh water forcing,” *Climate dynamics*, vol. 51, no. 4, pp. 1333–1350, 2018.
- [8] X. Chen and K.-K. Tung, “Varying planetary heat sink led to global-warming slowdown and acceleration,” *Science*, vol. 345, no. 6199, pp. 897–903, 2014.
- [9] D. Edwards, L. Emmons, D. Hauglustaine, D. Chu, J. Gille, Y. Kaufman, G. Pétron, L. Yurganov, L. Giglio, M. Deeter, *et al.*, “Observations of carbon monoxide and aerosols from the terra satellite: Northern hemisphere variability,” *Journal of Geophysical Research: Atmospheres*, vol. 109, no. D24, 2004.
- [10] T. P. Barnett, D. W. Pierce, K. M. AchutaRao, P. J. Gleckler, B. D. Santer, J. M. Gregory, and W. M. Washington, “Penetration of human-induced warming into the world’s oceans,” *Science*, vol. 309, no. 5732, pp. 284–287, 2005.
- [11] M. Dima and G. Lohmann, “A hemispheric mechanism for the atlantic multidecadal oscillation,” *Journal of Climate*, vol. 20, no. 11, pp. 2706–2719, 2007.
- [12] W. Liu, S.-P. Xie, and J. Lu, “Tracking ocean heat uptake during the surface warming hiatus,” *Nature communications*, vol. 7, p. 10926, 2016.
- [13] S. Levitus, J. I. Antonov, T. P. Boyer, O. K. Baranova, H. E. Garcia, R. A. Locarnini, A. V. Mishonov, J. Reagan, D. Seidov, E. S. Yarosh, *et al.*, “World ocean heat content and thermosteric sea level change (0–2000 m), 1955–2010,” *Geophysical Research Letters*, vol. 39, no. 10, 2012.
- [14] L. Zanna, S. Khatiwala, J. M. Gregory, J. Ison, and P. Heimbach, “Global reconstruction of historical ocean heat storage and transport,” *Proceedings of the National Academy of Sciences*, vol. 116, no. 4, pp. 1126–1131, 2019.
- [15] M. A. Balmaseda, K. E. Trenberth, and E. Källén, “Distinctive climate signals in reanalysis of global ocean heat content,” *Geophysical Research Letters*, vol. 40, no. 9, pp. 1754–1759, 2013.
- [16] V. Gladkikh and R. Tenzer, “A mathematical model of the global ocean saltwater density distribution,” *Pure and Applied Geophysics*, vol. 169, no. 1-2, pp. 249–257, 2012.